Copyright © 1998, by the International Council of the Aeronautical Sciences (ICAS)
and the American Institute of Aeronautics and Astronautics, Inc.

A98-31535

ICAS-98-3,1,4

INSTANTANEOUS PLIF MEASUREMENT OF SPECIES MOLE-FRACTION IN A VARYING TEMPERATURE SUPERSONIC FLOW

J.S. Fox, P.M. Danehy, and A.F.P. Houwing
Department of Physics, Faculty of Science, Australian National University, ACT 0200, Australia

Abstract

A theoretical model for instantaneous PLIF measurements of mole fraction in a shock tunnel flow with pressure gradients and large temperature variations is presented. The model determined the optimum excitation frequency which provided PLIF signal intensity proportional to freestream mole fraction. Experimental PLIF images of a two-dimensional slot scramjet injector with and without hydrogen fuel injection were obtained. Using the theoretical modelling, the injection image was corrected so that intensity directly corresponded to the freestream mixture fraction.

Introduction

Scramjets[1] have long interested researchers in the field of high-speed aerospace vehicles, as they are the only existing candidate for an air-breathing engine capable of operating at high supersonic and hypersonic speeds. They will most likely power the new generation of aerospace vehicles, significantly reducing space launch and international travel costs. One of the challenges associated with the design of a successful prototype scramjet is to achieve a sufficiently high degree of mixing between the fuel and air streams so that the injected fuel undergoes combustion prior to its expulsion from the vehicle. This study focuses on the development of a non-intrusive method to assist analysis of the mixing efficiencies of different scramjet injectors.[2]

The flow produced by a free-piston shock tunnel is a suitable environment for testing the performance of such engines and studying the processes of mixing and combustion close to their proposed operating conditions. The experiments for this study are being conducted using flows produced in the Australian National University's T3 free-piston shock tunnel facility.[3]

Many traditional line-of-sight methods have been used to visualise the flow in the scramjet including Schlieren, shadowgraph,[4] and interferometry.[5] However, these methods are unable to resolve flow variations along the light's path. In contrast, planar laser-induced fluorescence (PLIF) is suitable for both qualitative flow visualisation and quantitative measurements of complex three-dimensional flowfields. This technique provides species and quantum-state specific information with extremely good spatial and temporal resolution.

PLIF involves illuminating the flow with a thin sheet of laser light tuned to excite electronic transitions in a chemical species in the flow, in our case nitric oxide (NO). The fluorescence induced by this illumination is focussed onto an intensified charge-coupled device (ICCD) camera producing an image of fluorescence intensity in that region. With judicious choice of transition and a sophisticated analysis, the technique can yield measurements of temperature,[6] pressure,[7] or velocity.[8] It is also possible to obtain the species concentration distribution across the illuminated plane.[9]

Quantitative PLIF measurements often involve combining a number of images to obtain a result. For example, at least two images are required for many temperature measurement strategies, as the temperature is obtained by taking a ratio of images. Time-averaged fuel mole fraction images have been obtained with planar laser-induced iodine fluorescence.[10] However, the present flow is highly turbulent and therefore non-repeatable in detail. Consequently, techniques which rely on detailed repeatability are not suitable for quantitative measurements.

The work reported here centres around attempts to make quantitative measurements of the mole fraction in the presence of pressure gradients and large temperature variations. In this paper we demonstrate this method by investigating a two-dimensional slot injector, called the plane-base injector, injecting fuel into a co-flowing freestream at a Mach number of 4.

PLIF Theory

The PLIF signal is a function of temperature, pressure, mole fraction and a number of other known experimental parameters and is written as[11]

$$S_f = \frac{E_p}{A_{las}} \frac{\chi_a P}{kT} \sum_i [f_{J''} B g] \left(\frac{A}{A+Q} \right) C_{opt} \qquad (1)$$

where the summation is over all transitions; E_p is the laser energy per pulse; A_{las} is the cross-sectional area of the laser sheet; χ_a is the mole fraction of the absorbing species; P is the pressure; k is the Boltzmann constant; T is the temperature; $f_{J''}$ is the Boltzmann fraction of the absorbing state, which has rotational quantum number J''; B is the Einstein coefficient for absorption;

Copyright © 1998 by ICAS and AIAA. All rights reserved

Copyright © 1998, by the International Council of the Aeronautical Sciences (ICAS)
and the American Institute of Aeronautics and Astronautics, Inc.

g is the overlap integral; A is the effective rate of spontaneous emission for all directly and indirectly populated states; Q is the total collisional quenching rate of the electronic excited state; and C_{opt} is the efficiency with which photons emitted from the gas are converted to photoelectrons, which depends on the collection optical arrangement, spectral filtering, temporal gating, photocathode quantum efficiency, and intensifier gain. The term $\frac{A}{A+Q}$ is known as the fluorescence yield, ϕ.

The PLIF signal, as defined in equation (1), has both explicit and implicit dependencies on temperature and pressure. Implicit temperature dependencies enter the signal equation through the Boltzmann fraction, the spectral overlap integral and the quenching. Pressure dependence is implicit in the overlap integral and the quenching. These terms are detailed below.

The Boltzmann fraction, $f_{J''}$, expresses the population of rotational levels in relation to the temperature. It is given by[12]

$$f_{J''} = (2J'' + 1) \exp\left(\frac{-E}{kT}\right), \qquad (2)$$

where J'' is the rotational quantum number of the lower rotational level and E is its energy.

The spectral overlap integral,[13]

$$g = \int_0^\infty g_l(\nu_l, \Delta\nu_l) g_a(\nu_a, \Delta\nu_a) d\nu, \qquad (3)$$

determines the overlap between the laser spectrum and a particular transition. The parameter, g_l, is the spectral profile of the laser; g_a is the absorption line shape, assumed to be a Voigt profile; ν_l is the laser frequency; $\Delta\nu_l$ is the laser linewidth; ν_a is the absorption line frequency; and $\Delta\nu_a$ is the absorption linewidth. The functions g_l and g_a are normalised so that their individual integrals over all frequencies equal 1. Shifts and broadening of transitions due to pressure and temperature are taken into account in the integral of the absorption lineshape.[14] Due to the geometry of the flow, Doppler shifts are expected to be small and are neglected in this analysis.

Quenching depends on both pressure and temperature, as well as the species present in the flow:[11]

$$Q = \langle v_{NO} \rangle \langle\langle \sigma \rangle\rangle \left(\frac{P}{kT}\right) \qquad (4)$$

where $\langle v_{NO} \rangle = \sqrt{8kT/\pi m_{NO}}$; m_{NO} is the molecular mass of NO and the total electronic quenching cross-section is given by

$$\langle\langle \sigma \rangle\rangle = \sum_p \chi_p \sqrt{1 + m_{NO}/m_p} \langle\langle \sigma_p \rangle\rangle. \qquad (5)$$

The summation in equation (5) is over all perturbing species p; χ_p, m_p and $\langle\langle \sigma_p \rangle\rangle$ are the mole fraction, molecular mass and quenching cross-section of the perturbing species, respectively.

An understanding of the implicit temperature and pressures dependencies described by equations (2) - (5) is important in developing a technique that is capable of instantaneous mixture fraction imaging with minimal temperature and pressure sensitivity. These equations have been used to compute PLIF signal intensities for comparison with supersonic shock-layer experiments previously performed in our laboratories. Agreement with experimental measurements was excellent, lending support for our use of the PLIF model in this analysis.[15]

χ_{NO} imaging

With the majority of PLIF experiments it is best to tune to an isolated line, ensuring that neighbouring lines do not contribute to the PLIF signal. This simplifies quantitative analysis. However, to measure the mole fraction directly, a strategy must be devised to minimise the temperature and pressure dependence of the signal. Several authors have achieved this temperature independence by exciting overlapping transitions with the same laser pulse. For example, by making some assumptions and simplifying the parameters in the signal equation, Clemens[16] achieved a fluorescence intensity that was directly proportional to the mole fraction of NO. However, the temperature range of his work (140-270K) was far smaller than ours (150-1200K) and his simplifying assumptions are not valid for our choice of gases, making it more difficult to obtain the direct proportionality of the PLIF signal to the mole fraction of NO.

The aim of this work is to produce signal proportionality to NO mole fraction, that is, $S_f \propto \chi_{NO}$. From equation (1), this can be satisfied if the term

$$K \equiv \frac{E_p}{A_{las}} \frac{P}{kT} \sum_i [f_{J''} Bg] \left(\frac{A}{A+Q}\right) C_{opt} \qquad (6)$$

is constant, independent of temperature and pressure.

For the purposes of calculation, it was assumed that the only variation in temperature was due to the mixing of cold fuel with hot freestream gases. The temperature was then calculated using an enthalpy balance:[17]

$$T_{mix} = \frac{\left[\chi_{fuel} T_{fuel} + (1 - \chi_{fuel}) \frac{c_{p,\infty}}{c_{p,fuel}} T_\infty\right]}{\left[\chi_{fuel} + (1 - \chi_{fuel}) \frac{c_{p,\infty}}{c_{p,fuel}}\right]}. \qquad (7)$$

The subscripts, $fuel$, ∞, and mix refer to the pure fuel stream, pure free stream, and a mixture of the two respectively; and c_p is the specific heat of the streams. Therefore, the temperature in the calculation relates to how much fuel and freestream gas are in a particular part of the flow: the more fuel present, the closer the

Copyright © 1998, by the International Council of the Aeronautical Sciences (ICAS)
and the American Institute of Aeronautics and Astronautics, Inc.

temperature is to that of the fuel and vice versa for the freestream.

There were a number of variables to optimise in designing the experiment: the operating conditions, the gas compositions, and the frequency and linewidth of the laser.

The operating conditions were chosen based on fluid mechanical requirements. We wanted to use predominantly N_2 freestream and mostly H_2 fuel so that we could analyse mixing without the complication of combustion. A Mach number of 4 was chosen for the test section. This produced a temperature and pressure for the freestream gas in the test section of 1200 K and 50 kPa, respectively. The operating conditions of the injector were chosen so that the fuel jet was neither over- nor underexpanded. This resulted in a temperature and pressure at the exit of the injector of 150 K and 50 kPa, respectively.

The freestream gas compostion was controlled by the amount of NO required in the test section. The amount of NO was determined by the maximum tolerable absorption and the required quench rate, Q. Absorption was limited to 2% cm^{-1} to obtain relatively uniform images. This gave an upper bound to the amount of NO present in the test section. If the amount of the quenching species (O_2 and N_2) is chosen such that $Q \gg A$ (see expression (6)), this ensures that the implicit pressure dependence in the quenching cancels out the explicit pressure dependence of the PLIF signal. Another trade-off occurs here: if the quenching is too high then the signal is small whereas if the quenching is too low then the signal is dependent on pressure. The chosen composition for the shock tube gas was 98% N_2 with 2% O_2. When shock heated, the mixture of O_2 and N_2 produced an amount of NO in the freestream which gave good signal and the correct amount of quenching with $\leq$2% cm^{-1} absorption.

We equated the quench rate in the freestream and fuel regions so that the value of quenching was approximately the same for all T_{mix}. This resulted in the fuel being a mix of a small amount of CO_2, as the quencher, in H_2. CO_2 and CO were both considered when deciding the fuel quencher. CO_2 was chosen because it is non-toxic and has a higher quenching cross-section; [17] therefore, compared to CO, less of it is needed and the fuel can be approximated by pure H_2 when considering its fluid dynamical behaviour.

The choice of laser excitation frequency was also very important in ensuring that expression (6) remains as constant as possible. Different transitions must be excited by the laser to reduce the temperature dependence of expression (6). The Boltzmann fraction, $f_{J''}$, is very different for low- and high-J lines. Low-J transitions are more populated at low temperatures, while high-J lines are more populated at high temperatures. If the laser is tuned to a frequency which overlaps both low- and high-J lines then this will produce a value for expression (6) over a range of T_{mix} that is more constant than that produced by tuning to a single, isolated line. Once the excitation frequency is chosen, the absorption must be calculated again to check that it is still $\leq$2% cm^{-1}.

If this is the case, the only parameter left to adjust is the laser linewidth. The best linewidth is one that is sufficiently broad in order to overlap a number of transitions.

A FORTRAN code was written to evaluate expression (6) over a specified frequency range and determine the optimum excitation frequency which keeps expression (6) as constant as possible.

Discussion of specific flow geometry

Figure (1) shows a schematic of the flow over a two-dimensional slot scramjet injector without fuel injection. The injection slot is 1.06 mm in height and the total injector height is 8 mm. The flow is uniform in the freestream, and expands around the base of the injector on both upper and lower surfaces. At the base of the injector a region of very hot, low-pressure separated flow forms. This low speed recirculation region interacts with the high speed inviscid region via the separated boundary layer which lies between them.

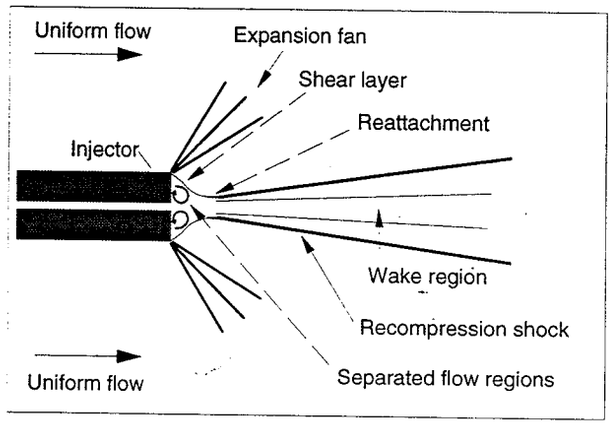

Figure 1. Schematic of the flow over a two-dimensional slot scramjet injector. This case is for non-injection.

After its expansion around the base, a recompression shock forces the flow to move parallel to the freestream again. The flow between the recompression shocks is at approximately constant pressure, since pressure can be considered to be approximately constant across a slowly growing shear layer. A wake region, having nearly the same properties of the boundary layer formed on the injector, is in the middle of the recompression shocks. The flow in the wake is hot and travelling slowly, while the flow between the wake

Copyright © 1998, by the International Council of the Aeronautical Sciences (ICAS)
and the American Institute of Aeronautics and Astronautics, Inc.

and the recompression shocks is relatively cooler and faster. Therefore, the region between the recompression shocks has a uniform pressure but varying temperature, velocity and density.

When fuel is injected, the flow is qualitatively similar but the recompresseion shocks are further apart and the fuel jet issues into the wake region.

Experiment

The experiments were performed using the ANU's T3 free piston shock tunnel. A 125 mm exit-diameter conical nozzle with a 35 mm throat-diameter was used to produce the required flow Mach numbers. Freestream conditions with a pressure of 50 kPa, a temperature of 1200 K and Mach number of 4.3 were produced. The 2% O_2 and 98% N_2 test gas in the shock tube produced approximately 1.6% NO, 1.2% O_2, 0.06% O, with a balance of N_2 in the test section (calculated using the computer code STUBE.[18]) As discussed above, the injected fuel was at a pressure of 50 kPa and a temperature of 150 K, giving a Mach number of 1.7. The fuel gas contained 0.3% CO_2 with a balance of hydrogen.

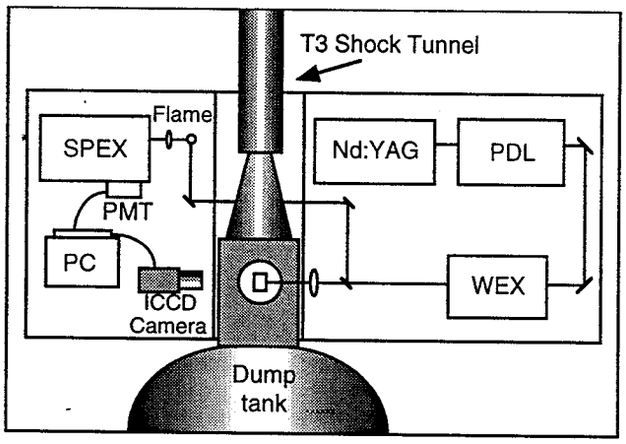

Figure 2. Schematic of the experimental arrangement as viewed from above: Nd:YAG is the laser which pumps the PDL which stands for pulsed dye laser; WEX stands for wavelength extender and is used to frequency-double and mix the light; SPEX stands for spectrometer; and PMT stands for photomultiplier tube. The UV laser sheet is directed down into the test section using a mirror, as shown.

A schematic of the experimental arrangement is shown in Figure (2). The operation of the shock tunnel is described by Stalker.[19] Before firing the tunnel, the laser was tuned to a particular NO transition and pulsed at a fixed repetition rate. The recoil of the tunnel initiated an electronic trigger which stopped the laser from continuously triggering and, with a preset delay, triggered the injection system. A transducer in the nozzle reservoir region registered the shock reflection from the end of the shock tube and the laser and camera systems were triggered 1.4 ms later. This delay corresponded to the time in which there was a steady flow.

PLIF Excitation and Detection

Light from a Nd:YAG laser at a wavelength of 1064 nm passed through a frequency-doubling crystal producing 532 nm light which pumped a dye laser operated with a mix of Rhodamine 590 and 610 laser dyes. The dye laser output light at 574 nm which was frequency-doubled and then mixed with the residual 1064 nm light to produce UV light at 226 nm. This light was used to excite transitions in the $A^2\Sigma^+ \leftarrow X^2\Pi(0,0)$ band of NO. Part of the beam was split off and used to monitor the laser energy and for wavelength calibration by passing it through a flame; the LIF from the flame was imaged onto a spectrometer and detected by a photomultiplier tube. Each pulse of the laser usually produced about 1 mJ of energy. A low pressure, room temperature LIF spectrum determined an upper limit to the linewidth of 0.9 ± 0.1 cm^{-1}. When injection-seeding the Nd:YAG laser, the laser linewidth was observed to be 0.5 ± 0.1 cm^{-1}.

The UV light was formed into a sheet with a 400 mm focal length cylindrical lens, then focussed with a 500 mm focal length spherical lens to a thickness of approximately 600 μm. A mask before the test section shortened the width of the beam from approximately 60 mm to 30 mm. This ensured a relatively uniform beam profile passed through the test section to excite the chosen transition of NO.

The fluorescence was captured normal to the direction of the laser sheet on a cooled ICCD camera. A UG-5 Schott glass filter was used to spectrally filter the fluorescence to remove any elastic scatter. A dye cell was used to monitor the energy variation in the laser sheet profile which was captured on a CCD camera simultaneously with the PLIF image of the flow. This profile was later used for correction of the image.

Results and Discussion

Line selection

Calculations done over the entire A-$X(0,0)$ NO spectrum determined that the optimal laser frequency was at 44282.38 cm^{-1}, centred on the $^pP_{11}(27)$ transition. Figure (3) shows the contributions to expression (6), from all the lines overlapped by the laser, for increasing amounts of freestream gas. The sum of the contributions is shown by the bold line.

Though a number of lines contribute to the final result, the most dominant are the $^pP_{11}(27)$, $^qQ_{22}(24)$ and $^sR_{21}(8)$ transitions. It is these three transitions that most clearly show the effect of the Boltzmann fraction on the signal: the $^sR_{21}(8)$ has a high signal for low temperatures, while the $^pP_{11}(27)$ and $^qQ_{22}(24)$ transitions have a high signal for higher temperatures. When

Copyright © 1998, by the International Council of the Aeronautical Sciences (ICAS)
and the American Institute of Aeronautics and Astronautics, Inc.

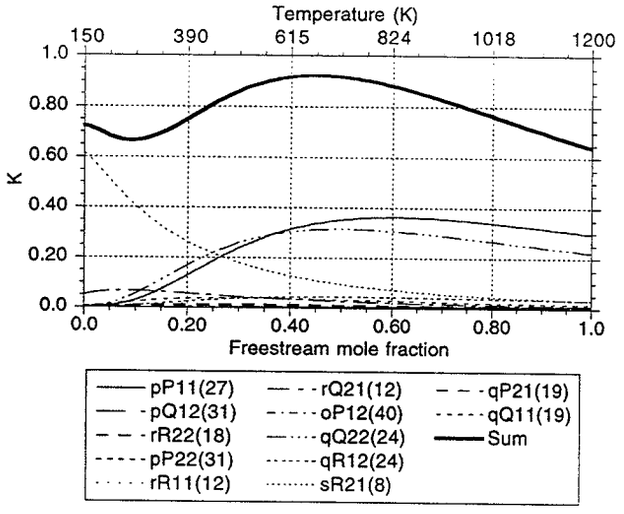

Figure 3. Contribution of individual transitions to the total PLIF signal. K is defined by expression (6).

summed together these produce a signal that is proportional to the mole fraction of NO, as desired.

PLIF signal intensity variation for pressures of 10, 30 and 50 kPa is shown in Figure (4). The signal changes only slightly even though pressure is increased fivefold, indicating that the PLIF signal is nearly independent of pressure. To further reduce this pressure dependence, the quench rate could be made higher, at the cost of reduced signal. However, over the entire pressure and temperature range we achieve $S_f \propto \chi_{NO}$ to within ±12%.

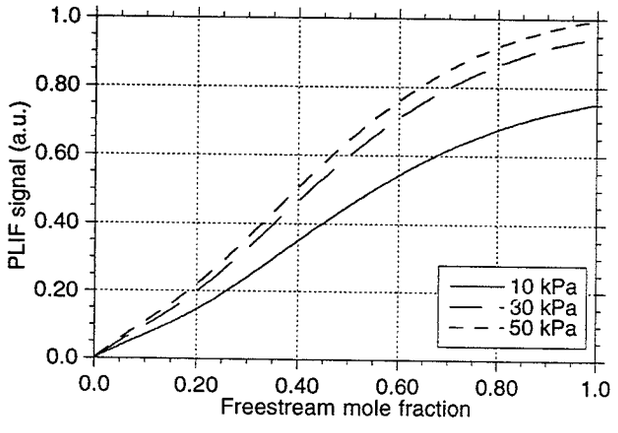

Figure 4. PLIF signal intensity variation with pressure.

The PLIF signal is shown in Figure (4) to be a monotonic function of fuel mole fraction. Therefore, we can use the theoretical modelling to convert experimental PLIF images to a quantitative measure of fuel mole fraction.

Since the freestream is at a pressure of 50 kPa and the base-flow region is at a pressure of 10 kPa, the mixed region is expected to be at a pressure of 30 kPa on average. This is the value that will be used in calculations to convert PLIF images to fuel mole fraction. A cubic polynomial was fitted to the 30 kPa signal trace. The result is shown in Figure (5).

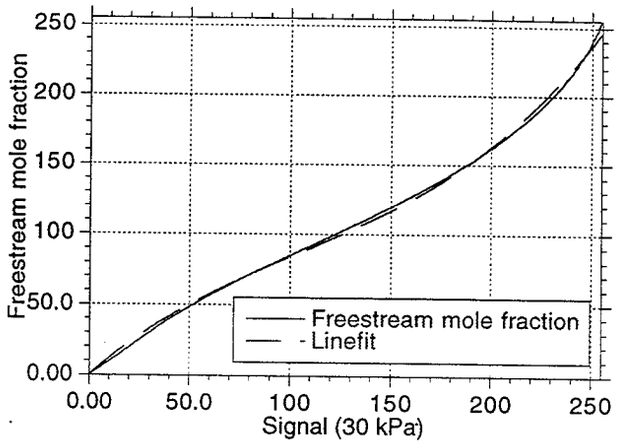

Figure 5. Cubic polynomial linefit to 30 kPa signal. This will be used to convert PLIF images to freestream mole fraction.

This figure shows the freestream mole fraction as a function of the PLIF signal intensity. The axes have been scaled to 255 to make this conversion a one-step process as the pixel values in the images will vary from 0 to 255. The cubic polynomial linefit has been chosen to convert PLIF signal to fuel mole fraction because it is a good fit to the theoretical signal for 30 kPa.

Experimental Results

Experimental images are shown in Figures (6) and (7). Both images show the same injector. Flow is from left to right. The laser sheet comes from the top, producing the shadow region beneath the injector, at the left of the image.

Figure (6) is a non-injection image. All the flow features are due entirely to the freestream passing over the injector. The expansion around the base of the injector results in a drop in pressure and temperature and causes a decrease in PLIF signal intensity in this region. Recompression shocks force the flow to again travel parallel to the freestream and can be seen quite clearly in the centre of the image. The increase in pressure and temperature across this shock causes the signal to increase. Note that the temperature and pressure changes in these regions are not due to mixing.

As discussed above, according to the fluid mechanical considerations, the pressure is approximately constant between the recompression shocks. The temperature is expected to vary considerably in this region. However, contrary to our original assumption, here the temperature effects are not the result of fuel and air mixing. Rather, the temperature variations are a result of the different flow velocities. Nonetheless, the

Copyright © 1998, by the International Council of the Aeronautical Sciences (ICAS)
and the American Institute of Aeronautics and Astronautics, Inc.

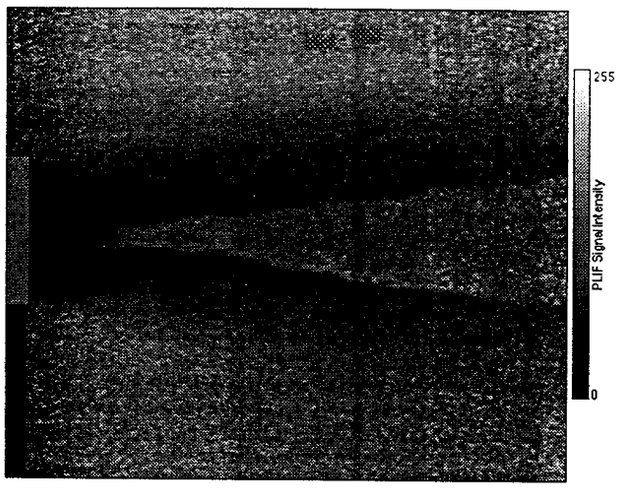

Figure 6. PLIF image of a two-dimensional slot injector without fuel injection. The injector's position is shown by the grey mask at the left of the image. The scale to the right indicates the PLIF signal intensity: black corresponds to low PLIF signal intensity and white to high PLIF signal intensity.

relatively uniform signal in this region provides evidence that our excitation method is insensitive to temperature. Outside the compression shocks, the signal intensity varies markedly due to the larger pressure and temperature changes. The region of validity of our PLIF model, then, is limited to the region between the recompression shocks.

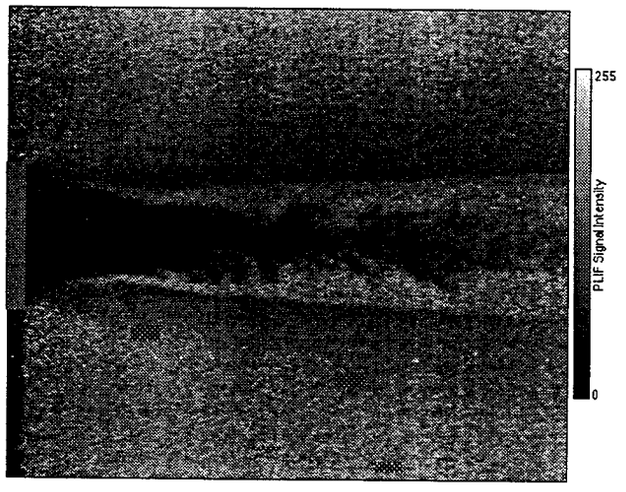

Figure 7. PLIF image of a two-dimensional slot injector with fuel injection. The injector's position is shown by the grey mask at the left of the image. The scale to the right indicates the PLIF signal intensity: black corresponds to low PLIF signal intensity and white to high PLIF signal intensity.

Figure (7) is an injection image. The dark central area is the region of fuel injection; the bright areas at the top and bottom of the image are pure freestream; and in between are two mixing layers. Injection of fuel into the flow causes the recompression shocks to be pushed further apart. The expansions around the injector can still be seen, but they are smaller due to the change in position of the recompression shocks. Turbulent eddies can clearly be seen in the mixing layers. The mixing layers grow in width as the flow moves downstream, indicating that the freestream and fuel are beginning to mix.

Image analysis

The cubic polynomial linefit in Figure (5) was used to correct the region between the two recompression shocks of the injection image of Figure (7) for mole fraction. The result of this correction is shown in Figure (8). The injector is at the left of the image and flow is from left to right.

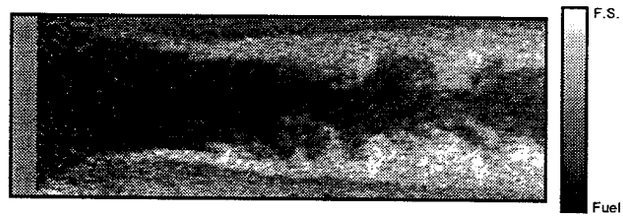

Figure 8. Quantitative image of freestream and fuel mole fraction for the plane-base injector. The injector's position is shown by the grey mask at the left of the image. The scale to the right indicates the amount of freestream gas.

Note that the assumptions of the model are only valid in the region between the two recompression shocks, which can be seen at the top and bottom of Figure (8). The scale to the right of the image indicates the relationship between the image intensity and the level of mixing. A black area indicates pure fuel, a white area indicates pure freestream, and the grayscale indicates some amount of mixing. The penetration of the freestream into the fuel jet increases as the flow progresses downstream, as does the width of the mixing layer.

Conclusion

A theory for instantaneous PLIF imaging of mole fraction in a flow with pressure gradients and large temperature variations has been presented. The aim was to achieve PLIF signal intensity proportional to mole fraction, independent of temperature and pressure.

The PLIF signal was strongly dependent on the gas compostion, laser excitation frequency and linewidth. Gases with sufficiently high quenching cross-section to achieve $Q \gg A$, reducing the signal's pressure dependence, were chosen. The laser excitation frequency and linewidth were chosen to overlap a number of transitions with both low- and high-J rotational numbers. This assisted in removing the temperature dependence of the signal. Optimising the parameters in the PLIF

Copyright © 1998, by the International Council of the Aeronautical Sciences (ICAS)
and the American Institute of Aeronautics and Astronautics, Inc.

signal equation produced a proportionality to mole fraction within ±12%, according to theory.

Experimental PLIF images of a plane-base injector with and without fuel injection were obtained using the optimum laser frequency specified by the theory. The injection image was corrected using a cubic polynomial linefit to the theoretical 30 kPa PLIF signal intensity curve. Intensity in the resulting image was then proportional to the mole fraction. However, further work on validating this method needs to be completed before we can use it with complete confidence.

Acknowledgements

This research has been financially supported by the Australian Research Council. The authors would like to thank Paul Walsh for the contribution of his technical expertise to this project. The contributions of Matt Gaston and Phil Palma are also gratefully acknowledged.

References

1. E. T. Curran, W. H. Heiser, D. T. Pratt, "Fluid Phenomena in Scramjet Combustion Systems", Anual Review of Fluid Mechanics, Vol. 28, pp323-360, 1996.
2. M. J. Gaston, N. R. Mudford and A. F. P. Houwing, "A Comparison of Two Hypermixing Fuel Injectors in a Supersonic Combustor", AIAA 36th Aerospace Sciences Meeting and Exhibit, Paper 98-0964, Reno, NV, Jan 1998.
3. R. J. Stalker, "The Australian National University Free Piston Shock Tunnel T3 Facility Handbook", Internal Report, Document No. 85/4/233.
4. T. J. McIntyre, A. F. P. Houwing, P. C. Palma, P. A. B. Rabbath, J. S. Fox, "Optical and Pressure Measurements in Shock Tunnel Testing of a Model Scramjet Conbustor", Journal of Propulsion and Power, Vol. 12, No. 3, 1997.
5. R. J. Stalker, R. G. Morgan and M. P. Netterfield, "Wave processes in scramjet thrust generation", Vol. 71, pp 63-67, 1988.
6. B. K. McMillin, J. L. Palmer and R. K. Hanson, "Temporally resolved, two-line fluorescence imaging of NO temperature in a transverse jet in supersonic cross flow", Appl. Opt. 32, 7532 (1993).
7. B. Hiller and R. K. Hanson, "Simultaneous planar measurements of velocity and pressure fields in gas flows using laser-induced fluorescence", Appl. Opt. 27, 33-48, 1988.
8. J. L. Palmer, B. K. McMillin and R. K. Hanson, "Planar laser-induced fluorescence imaging of velocity and temperature in shock tunnel free jet flow", AIAA Paper 92-0762 (1992).
9. A. Lozano, S. H. Smith, M. G. Mungal and R. K. Hanson, "Concentration measurements in a transverse jet by planar laser-induced fluorescence of acetone", AIAA Journal, Vol. 32, No. 1, pp 218-221, 1994.
10. J. D. Abbitt III, R. J. Hartfield and J. C. McDaniel, "Mole-fraction Imaging of Transverse Injection in a Ducted Supersonic Flow", AIAA Journal, Vol. 29, No. 3, pp 431-435. 1991.
11. P. H. Paul, J. A. Gray, J. L. Durant and J. W. Thoman, "Collisional Quenching Corrections for Laser-Induced Fluorescence Measurements of NO $A^2\Sigma^+$", AIAA Journal, Vol. 32 No. 8, pp 1670-1675, 1994.
12. Vincenti and Kruger, "Introduction to Physical Gas Dynamics", Robert E. Kreiger Publishing Co., 1965.
13. K. P. Gross, R. L. McKenzie, P. Logan, "Measurements of temperature, density, pressure, and their fluctuations in supersonic turbulence using laser-induced fluorescence", Expt in Fluids, Vol. 5, pp372-380, 1987.
14. M. D. DiRosa, "High-resolution line shape spectoscopy of transitions in the gamma bands of nitric oxide", PhD Thesis, Stanford, 1996.
15. P. M. Danehy, P. C. Palma, T. J. McIntyre, and A. F. P. Houwing, "Comparison of theoretical laser-induced fluorescence images with measurements performed in a hypersonic shock tunnel", 19th AIAA Advanced Measurement and Ground Testing Technology Conference, AIAA paper 96-2236, New Orleans, LA, 1996.
16. N. T. Clemens, "An experimental investigation of scalar mixing in supersonic turbulent shear layers", PhD Thesis, Stanford, 1991.
17. B. K. McMillan, "Instantaneous two-line PLIF temperature imaging of nitric oxide in supersonic mixing and combustion flowfields", PhD Thesis, Stanford, 1993.
18. I. M. Vardavas, "Modelling reactive gas flows within shock tunnels", Australian Journal of Physics, Vol. 37, pp157-177, 1984.
19. R. J. Stalker, "A Study of the Free-Piston Shock Tunnel", AIAA Journal, Vol. 3, No. 12, pp2160-2165, 1967.